New Amine Based Solvents for Acid Gas Removal

Yohann Coulier, Elise El Ahmar, Jean-Yves Coxam, Élise Provost, Didier Dalmazzone, Patrice Paricaud, Christophe Coquelet, Karine Ballerat-Busserolles

HAL Id: hal-01525924

https://minesparis-psl.hal.science/hal-01525924

Submitted on 22 May 2017

X. New Amine Based Solvents for Acid Gas Removal

Yohann COULIER[1,2,3], Elise EL AHMAR[3], Jean-Yves COXAM[1,2], Elise PROVOST[4], Didier DALMAZZONE[4], Patrice PARICAUD[4], Christophe COQUELET[3], Karine BALLERAT-BUSSEROLLES[1,2,3]

[1] *Clermont Université, Université Blaise Pascal, Institut de Chimie de Clermont-Ferrand, BP 10448, F-63000 CLERMONT-FERRAND, FRANCE*
[2] *CNRS, UMR 6296, Institut de Chimie de Clermont-Ferrand, F-63171 AUBIERE, FRANCE*
[3] *MINES ParisTech, PSL – Research University, CTP – Centre of Thermodynamics of Processes, F-77300 Fontainebleau, FRANCE*
[4] UCP, ENSTA ParisTech, Université Paris-Saclay, *France 828 Boulevard des Maréchaux, 91762 Palaiseau cedex, France.*

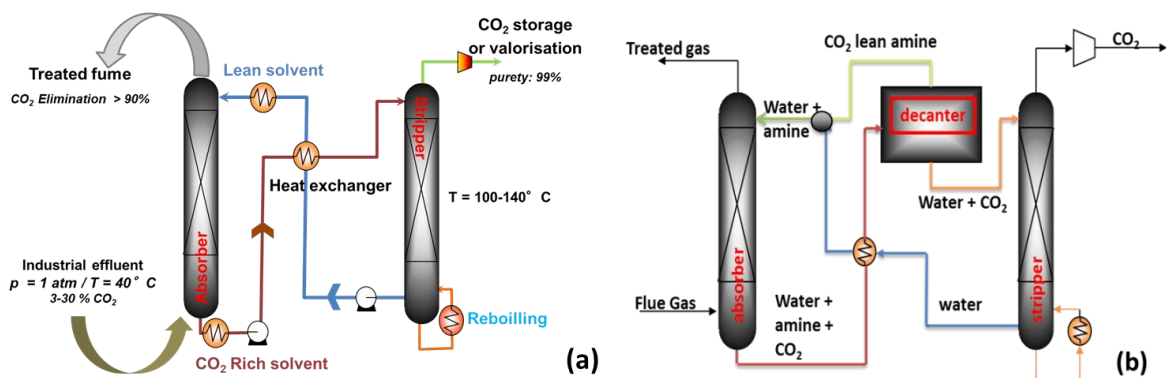Corresponding author: yohann.coulier@univ-bpclermont.fr

Abstract

Treatment and separation of multicomponent gases using absorption/desorption cycles in aqueous solutions is a very well-known and efficient method, used in natural gas treatment, biogas purification, greenhouse gas control … More specifically, the use of aqueous solutions of amine is used with benefit for CO_2 removal in mixed gases. However, the energetic cost of this method is highly expensive in carbon capture processes. A new class of amine is considered to decrease the cost of the regeneration: the demixing amines. These amines present a lower critical solution temperature that can be used with benefit in post-combustion processes. The LCST depends strongly on the chemical structure of the amine and on the presence and quantity of dissolved gas. The aim of this chapter is to evaluate the influence of physical absorbent, namely triethylengycol, on the liquid-liquid equilibria, and on the associated thermodynamic properties (vapor-liquid equilibria, heat capacities, densities, heat of solutions) of the solutions needed for design of the carbon capture process.

X.1 Introduction

Chemical absorption of acid gases by amine based solvents has found applications in a wide variety of industries including gas processing and the removal of CO_2 from synthesis gas in the production of hydrogen or ammonia. Other applications of this technology is the purification of biogas [1] or CO_2 removal from post-combustion gases in power plants [2].

The principle of the technology applied to carbon capture processes is based on selective absorption/desorption cycles of CO_2 in aqueous absorbents. A schematic view of the process is shown in figure X.1. The major problem with this process is the cost of the regeneration step that requires a lot of energy to be efficient. Although the process is well adapted and extensively used for natural gas treatment, the composition of the industrial effluents leads to a loss of energetic efficiency. It is thus necessary to adapt this process in order to reduce the energetic cost of the desorption step.

Figure X.1 : Schematic representation of the CO_2 separation process [3]; (a) classical alkanolamine based absorbents; (b) demixing solvents.

Demixing solvents were proposed as an option for CO_2 capture to reduce the energy consumption involved in the regeneration of the absorbent [4]. These new absorbent solutions are constituted of amines that are partially miscible with water, under specific conditions of temperature and gas loading [5]. In the absorber, the aqueous solution of amine remains monophasic and a large quantity of CO_2 is absorbed similarly to the process using MEA. By increasing the temperature in the decanter, the solution separates in two liquid phases, one amine phase containing almost no CO_2, and one aqueous phase containing chemically and physically absorbed CO_2. Since the solubility of the gas in the aqueous phase is smaller than in the original monophasic solution due to composition and temperature changes, the CO_2 in excess desorbs from the solution while the remaining CO_2 is contained in the water rich phase. As a result, only this part of the solvent is heated in the regeneration step of the separation process. The excess CO_2 from the decanter and the separated CO_2 from the stripper are then compressed and transported for being uses or stored in safe conditions.

In order to apply such a process, two important parameters have to be considered:

- The liquid-liquid phase separation should only occur in the decanter and has to be avoided in the absorber. For that purpose the temperature of phase separation needs to be bigger than the maximum temperature in the absorption column.
- The amine rich phase should contain as less water as possible. The process is efficient if most of the CO_2 not released in the decanter, remains dissolved in the aqueous phase. Thus the amine phase to be directly recycled in the absorber.

The DACOOTA project presented by Ballerat-Busserolles et al. [6] and Fandino et al. [7] deals with the understanding of thermodynamic equilibria in {amine + H_2O} and {CO_2 + amine + H_2O} systems which exhibit partial miscibility with water. This project is simultaneously supported by the French National Agency of Research (ANR, [ANR-12-IS09-0001]) and the Natural Sciences and Engineering Research Council of Canada (NSERC). The goal of this research project is to elucidate the structure-property relationships for the potential amines under investigation, determine phase diagrams with or without dissolved CO_2, develop thermodynamic models, and evaluate the capabilities of the selected solvents for CO_2 absorption. In this project, methods to determine liquid-liquid equilibria (LLE) in mixtures containing a well-controlled quantity of gas dissolved were developed in order to elucidate part of the questions concerning this process.

During the last years, the addition of a physical solvent in aqueous solutions of amines was considered to optimize some steps of the process [8]. For example, in order to prevent equipment corrosion in processes of CO_2 capture with aqueous amines solutions, the use of a co-solvent such as glycol have already been explored [9]. Benefits due to the replacement of a part of the water by a physical solvent are the reduction of the specific heat capacity of the absorbent, together with the decrease of amine degradation and the reduction of evaporation, lowering the cost of the separation process.

In order to design new operation units for CO_2 removal or to evaluate the retrofits of existing processes, it is important to investigate the thermophysical properties of the new demixing solvents containing physical co-solvents. This includes phase equilibrium measurements (vapor-liquid and liquid-liquid equilibria), as well as the study of transport and energetic properties. The knowledge of these thermophysical properties will allow the evaluation of the impact of addition of physical solvent on CO2 mass transfer. Moreover, CO_2 gas stream is not pure and contain other chemicals such as N_2, Ar, NO_x, and SO_2 in the case of post-combustion capture process or H_2 and SO_2 in case of pre-combustion process, and H_2S and mercaptans in

case of gas processing or biogas purification. The impacts of these other chemicals on the thermophysical properties and phase diagram need also to be investigated.

In this work, the thermodynamic properties of a new demixing solvent composed of an aqueous solution of piperidines, namely N-methylpiperidine (NMPD) or 2-methylpiperidine (2MPD), and a physical solvent, triethylene glycol (TEG), are reported. Relying on the thermodynamic representation of the process [6], the benefit of adding a co-solvent were investigated as follows:

- For the decantation step, the liquid-liquid equilibria (LLE) of {Amine – H_2O – TEG} systems with dissolved CO_2 were studied.
- For transport properties in the lines and energy cost of the heating, densities and heat capacities of solutions were investigated at different temperatures.
- For solvent recycling and evaporation concerns, vapor-liquid equilibra (VLE) measurements for different CO_2 loadings were performed on {Amine – H_2O – TEG} systems.
- For energetic aspects of absorption and regeneration, the enthalpies of solution of CO_2 in {Amine – H_2O – TEG} were determined.

A comparative and comprehensive study to determine the positive effects coming from the addition of a physical solvent on the demixing solvent is proposed for all the investigated properties.

X.2 Chemicals and Materials

N-methylpiperidine, 2-methylpiperidine, and triethylene glycol were used without further purification. Water was distilled and degassed before use (resistivity 18.2 MΩ·cm). Solutions were prepared by mass; uncertainty in mass fraction (w) is estimated to be less than $\pm\ 10^{-4}$. The solutions were stored in glass bottle in an opaque cabinet to prevent any photo-degradation. Suppliers, purities and CAS numbers of all chemicals used in this study are given in Table X.1.

Table X.1. Suppliers, CAS numbers and stated purities (mass fraction w) of chemicals used in this study.

Chemical	Suppliers	CAS Number	w
N-methylpiperidine (NMPD)	Sigma-Aldrich	626-67-5	99.9 %

[a]2-methylpiperidine (2MPD)	Sigma-Aldrich	109-05-7	98.3 %
Triethylene glycol (TEG)	Sigma-Aldrich	112-27-6	99.0 %
Carbon dioxide (CO_2)	Air Products	124-38-9	99.995 %

[a] racemate

X.3 Liquid-liquid equilibria

X.3.1 LLE in {methylpiperidines + H_2O} and {methylpiperidines + H_2O + CO_2}
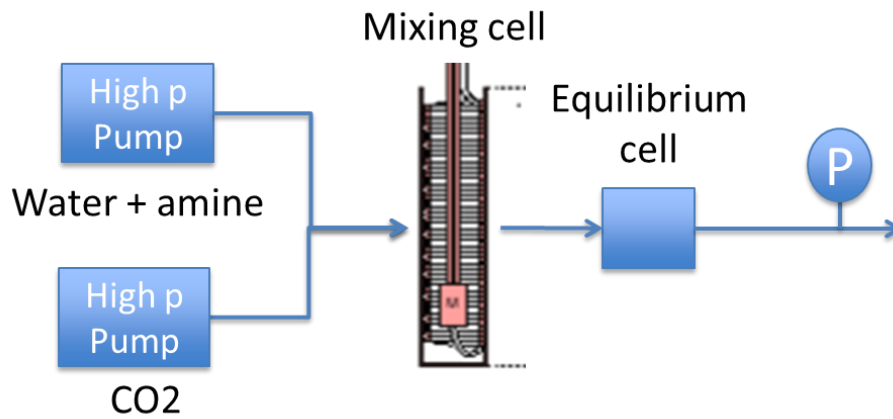
The LLE of the binary systems {NMPD – H_2O} and {2MPD – H_2O} have previously been studied by Coulier *et al.* [10] and Stephenson et al. [11]. An experimental technique recently developed by Coulier *et al.* [12] allows the determination of liquid-liquid equilibria with controlled quantities of dissolved CO_2. The LLE data were measured by Coulier *et al.* [12] using the cloud point method. It consists in determining the temperature at which a second liquid phase appears or disappears in a liquid system.

For solutions containing dissolved CO_2, two different apparatuses using the visual determination of the temperature of phase separation were set up depending on the range of temperatures investigated. The first apparatus is a visual phase equilibrium cell SPM20 from Thar instruments. The equipment features a high pressure chamber provided with pressure and temperatures sensors and a thick sapphire window that allows the visualization of the cloud point through a camera connected to a computer. The second cell, supplied by CTP Mines ParisTech is fully made of sapphire, allowing the visualization of the entire sample, instead of a limited zone. This cell is immerged in silicon oil cooling bath to extend measurements to temperatures below 273 K. The detailed characteristics of the apparatuses are given in table X.2.

Table X.2: characteristics of the visual cells used for cloud point measurements

	Equilibium cell	Sapphire cell
T (K)	Room T – 393	270 – 393
Control of T	Heat tape	Thermostatic bath
p (MPa)	1 – 400	1 – 80
Control of p	Buffer volume	Buffer volume
Inner volume (mL)	10 - 20 adjustable	5
Visualization of the sample	sapphire window	Full sample

Aqueous solutions of amine loaded with controlled quantities of CO_2 are prepared in a custom-made flow mixing cell. The overall experimental arrangement of the two systems is depicted in Figure X.2. The mixing cell is built with the same structure than the one developed at ICCF for enthalpies of solution measurements [13]. The mixing point consists in a Y piece, where two 1/16" stainless steel tubes are soldered on the top branches of the Y, while a unique tube containing the final mixture goes out from the bottom branch of the mixing point.

Figure X.2: Overall experimental set-up of liquid-liquid equilibrium cells for solutions containing dissolved gas.

The two fluids, CO_2 and the aqueous amine solution, are injected into the mixing cell supplied by two ISCO model 100 DM high-pressure syringe pumps. As the syringe pumps deliver constant volumic flow rates, they were regulated at a constant temperature of 298.15 K using a thermostatic bath in order to calculate accurately the composition of the aqueous solutions containing dissolved gas. The system pressure is maintained constant to 0.02 MPa using a buffer volume of 1 dm^3 equipped with a back pressure regulator and placed at the end of the flow line. The gas loading α (mol CO_2 / mol amine) of the mixture leaving the mixing unit was determined using the molar flow rates delivered by the two syringe pumps (Eq 1).
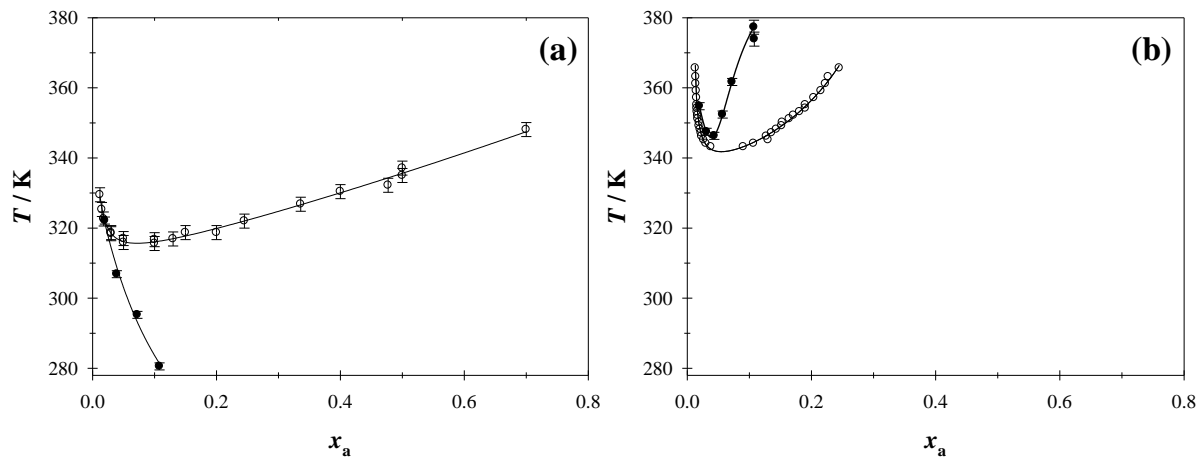
$$\alpha = \frac{\dot{n}_{CO2}}{\dot{n}_{amine}}$$

(1)

where $\dot{n}_{CO2}$ and $\dot{n}_{amine}$ are the molar flow rates of CO_2 and aqueous solution of amine respectively. To calculate the molar flow rates, the densities of the aqueous solution of amine and CO_2 are needed at the experimental conditions of temperature and pressure. The densities

of the solution as a function of the pressure were measured using an Anton Paar densimeter DMA HP. The densities of CO_2 were calculated using the equation of state from Span and Wagner [14]. Details on the calculation of the loading charge and its uncertainty are found in Arcis *et al.* paper [13]. The relative uncertainty on loading charge using this method is estimated to be less than 4%.

The same devices are used to measure temperature of phase separation for solutions without dissolved gas. In that case, the solutions are directly injected in the visual cell, without using the mixing cell prior to the entrance of the visual cell.

The procedure for the cloud point determination is the same independently of the system measured (visual isochoric method). Once the cell is entirely filled with the homogeneous solution (without any vapor phase), it is isolated from the pumps. Then the temperature in the cell is increased at a definite scanning rate (0.2 to 1 K/min) to find the tightest possible temperature interval in which the second phase appears. During this procedure, the cell is still connected to the buffer volume to avoid pressure increasing due to thermal expansion. The change in turbidity is detected visually. The uncertainty on the temperature of the cloud point was estimated from reproducibility tests and is less than $u(T) = 2K$, while uncertainty on such temperature determination for one experiment is $u(T) = 0.5$ K.

Figure X.3: Phase diagram, temperature versus mole fraction, for ternary mixtures of (a), {CO_2 –NMPD – H_2O} and (b), {CO_2 –2MPD – H_2O}, at constant loading charges: opened circle, $\alpha = 0$ [10, 11] and filled circle, $\alpha = 0.2$. Solid lines are smooth fitting lines.

The phase diagrams of the binary systems {NMPD – H_2O} and {2MPD – H_2O} were previously determined [10, 11] and the lower critical solution temperatures (LCST) were found to be 318 K for $x_{NMPD} = 0.07$ and 339 K for $x_{2MPD} = 0.05$ respectively.

Concerning the liquid-liquid phase diagrams of the binary systems illustrated in figure X.3, the behavior of the two methylpiperidines with water is very different. For example at 353 K, without CO_2, the water rich phase of the {NMPD – H_2O} system is poor in amine ($x_{NMPD}=0.005$) and the water content of the amine rich phase is rather small ($x_w = 0.2$). While at the same temperature, the water rich phase of the {2MPD – H_2O} system is rather poor in amine ($x_{2MPD}=0.017$) but the amine rich phase is highly rich in water ($x_w = 0.82$). Without CO_2, the phase diagrams of the binary systems show that using NMPD instead of 2MPD is more favorable for the demixing process.

At a constant gas loading charge of 0.2, the temperatures of phase separation decrease significantly with the addition of NMPD and reach 280 K for a composition of amine solution $x_{NMPD}=0.11$. Measurements were not feasible for more concentrated solutions, solutions due to the limits of temperatures of our techniques (270 K – 393 K). With 2MPD, the phase diagram with dissolved CO_2 is similar to the one without CO_2 up to $x_{2MPD}=0.046$. We do not observe any significant change of the lower critical end point. Moreover, a significant shrinkage of the immiscibility gap is observed. Finally, we can also notice that the "amine phase" is very rich in water. Those differences are mainly due to different chemical reactions occurring in the solution in the presence of CO_2 [12].
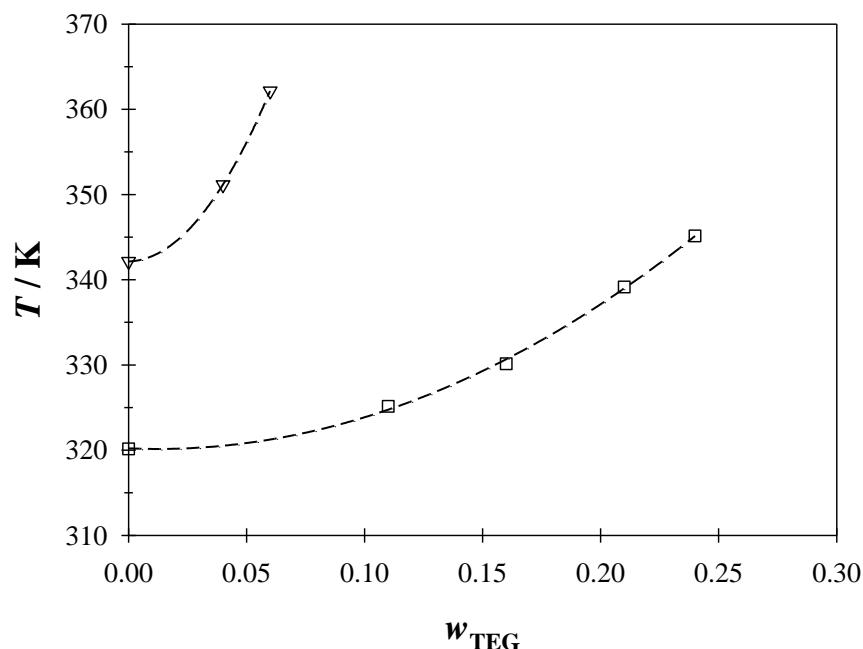
Considering those phase diagrams, none of these amines can reach the requirements of the proposed process with CO_2. The ideal system considering these methylpiperidines would be a compromise between the large phase diagram of NMPD and the temperature of phase separation obtained with 2MPD.

X.3.2 Liquid-Liquid Equilibria of ternary systems {Amine – H_2O – Glycol}

The addition of a physical solvent, triethylene glycol (TEG) was considered to increase the temperatures of phase separation of the mixtures, without changing the shape of the curve. A test study was then realized in the ternary liquid system {(N- or 2-)MPD – H_2O – TEG} to verify the influence of the TEG on the LLE.

The visual technique previously described was used to evaluate the influence of the glycol on the LLE at atmospheric pressure. For that purpose, increasing amounts of TEG were added to

aqueous solutions of NMPD and 2MPD with a starting amine composition w_a=0.2. The temperatures of phase separation for both systems are presented in Figure X.4.

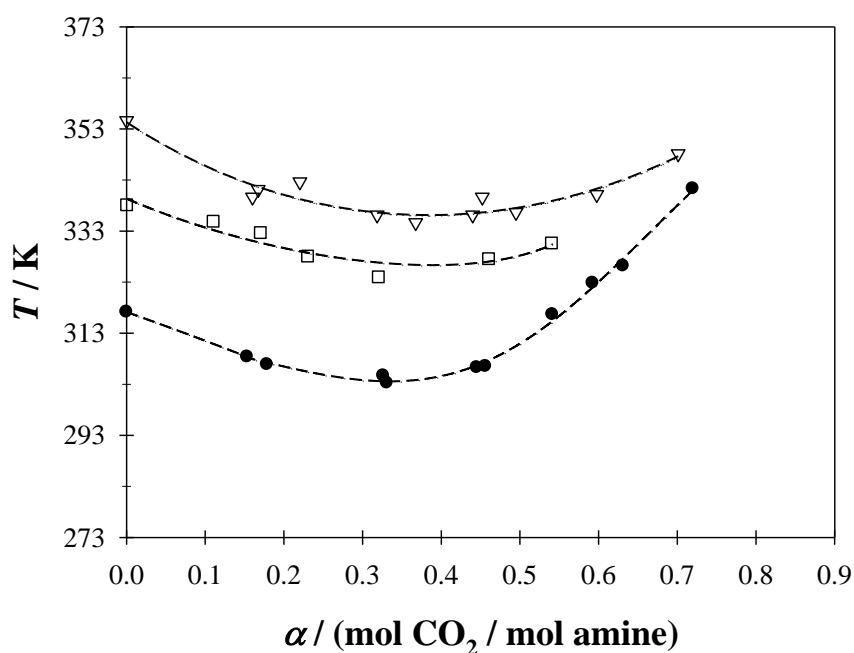Figure X.4: LLE of the ternary systems: □, {NMPD – H$_2$O – TEG} and J, {2MPD – H$_2$O – TEG}.

In an aqueous solution of 2MPD ($w_{2MPD} = 0.2$), the addition of small amounts of TEG leads to a sharp increase of the temperatures of phase splitting, limiting the amount of TEG to $w_{TEG} = 0.075$ due to the temperature range of the technique. For the ternary system {NMPD – H$_2$O – TEG}, phase separation temperatures are also rising while adding TEG. Nevertheless these temperatures stay low enough with a reasonable amount of physical solvent to be undertaken in the demixing process.

X.3.3 Liquid-Liquid Equilibria of the quaternary systems {CO$_2$ – NMPD – TEG – H$_2$O}

The influence of CO$_2$ on the phase diagram was then evaluated in mixtures containing NMPD and TEG. The liquid-liquid equilibrium data were determined at 0.5 MPa for two mixtures, {NMPD (20) – TEG (20) –H$_2$O (60)} and {NMPD (20) – TEG (30) –H$_2$O (50)}. Numbers in brackets denote the weight percent of each mixture component. Figure X.5 compares the phase diagrams of these two systems as a function of CO$_2$ loading charge with the one without TEG determined by Coulier *et al.* [12].

Figure X.5: Phase diagram, temperature versus loading charge, for quaternary mixtures of $\{CO_2 - NMPD - TEG - H_2O\}$: ●, $\{CO_2 - NMPD\ (20) - TEG\ (0) - H_2O\ (80)\}$; □: $\{CO_2 - NMPD\ (20) - TEG\ (20) - H_2O\ (60)\}$ and ▽, $\{CO_2 - NMPD\ (20) - TEG\ (30) - H_2O\ (50)\}$. Numbers in brackets denote the weight percent of each mixture component. Dash lines are smooth fitting lines.

As shown in section X.3.2, adding TEG to an aqueous solution of NMPD yields to an increase of the temperatures of phase separation. The shape of the LLE curves investigated with TEG is similar to the one obtained by Coulier *et al.* [12] without TEG. The main difference concerns the temperature of the lower critical end point which increases while adding TEG. However it is a very valuable benefit for the process with demixing solvent since temperatures of phase separation can be controlled by the quantity of physical solvent.

As the LLE regions are well controlled by adding TEG, measurements of the other thermodynamic properties of the mixtures were carried out, to provide additional information in case of a process development and to compare the capacity of such solvents with ones without TEG. From the previous results, NMPD appears to be the most promising amine for this application. Thermodynamic properties such as densities and heat capacities of mixtures containing this amine were determined

X.4 Densities and heat capacities of ternary systems $\{NMPD - H_2O - Glycol\}$

Densities and heat capacities are two essential thermodynamic properties that need to be measured to optimize separation processes. Indeed the densities drive part of the transport properties of the solutions, and heat capacities control the energetic cost resulting from heating during the process. Densities are also needed for any calculations of molar properties from volumetric measurements (solution composition in LLE or enthalpies of solutions containing CO_2, heat capacities…).
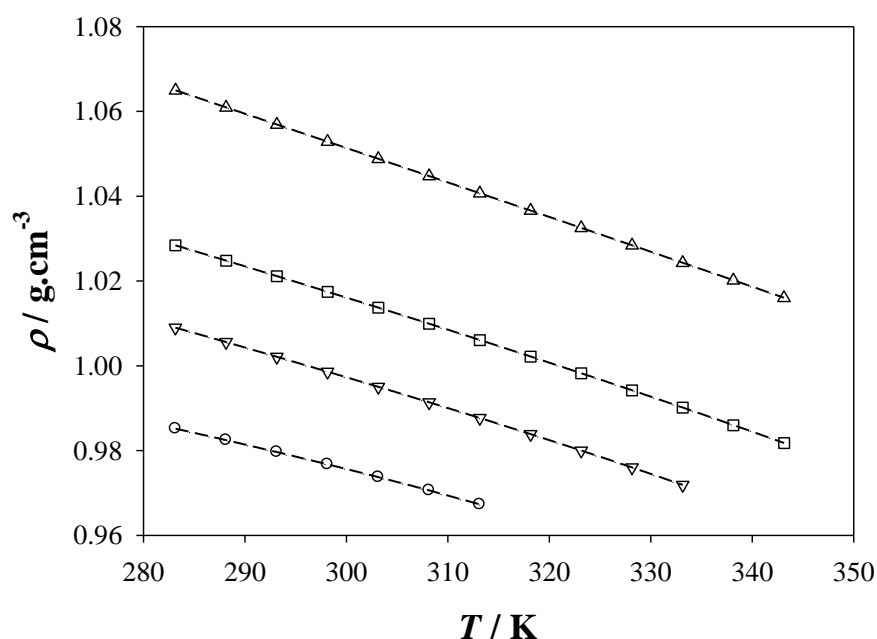
X.4.1 Densities

The densities of the ternary solutions {NMPD – H_2O – TEG} were measured at atmospheric pressure using an Anton Paar DMA 5000 density meter and the experimental procedure is given by Coquelet *et al.* [15]. Compositions in amine, water and TEG and the ranges of investigated temperatures are resumed in Table X.3. The range of temperature studied is limited by the LLE as measurements have to be realized for homogeneous one phase solutions. The range of studied temperature is then larger when adding TEG, as explained in chapter X.3.2.

Table X.3. Composition of the ternary systems {NMPD – H_2O – TEG} and temperature range investigated in the density study.

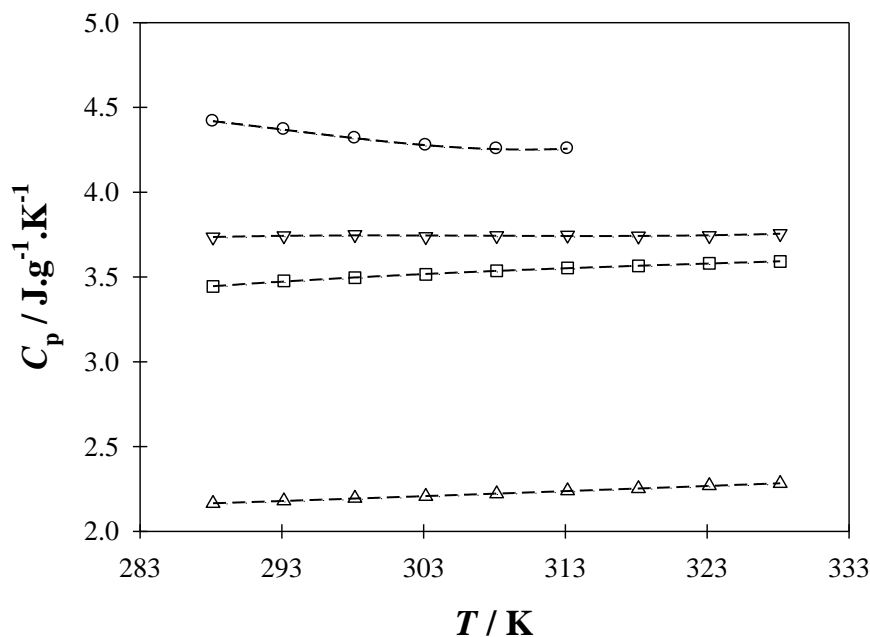| NMP	TEG	H_2O	T
	wt %		K
20	20	60	283–333
20	30	50	283–343
30	20	50	283–338
30	30	40	283–343
20	80	0	283–343
30	70	0	283–343
0	100	0	283–343
100	0	0	283–343
20	0	80	283–313
30	0	70	283–313

The influence of glycol on the densities of aqueous solution of NMPD is shown in Figure X.6. An increase of the densities is observed with the addition of TEG at all studied temperatures. The density of solutions decreases also when the temperature is increased. The curves are mostly shifted to the highest values of densities when TEG is added to the solution.

Figure X.6:.Densities of the ternary systems {NMPD (w %) – TEG (w %) – H_2O (w %)}. ○, {NMPD (20) – TEG (0) – H_2O (80)}; ▽, {NMPD (20) – TEG (20) – H_2O (60)}; □, {NMPD (20) – TEG (30) – H_2O (50)}; △, {NMPD (20) – TEG (80) – H_2O (0)}. Numbers in brackets denote the weight percent of each mixture component. Dash lines are smooth fitting

X.4.1 Specific heat capacities

The specific heat capacities of aqueous amine solutions were determined by using a differential scanning microcalorimeter from SETARAM, France (microSC) equipped with liquid C_p cells of 1 mL inner volumes. The detection is based on the Calvet principle. The experimental procedure is given by Coulier *et al.* [16]. First, a blank experiment is performed by filling both the sample and reference cells with nitrogen (N_2). Then, the sample cell is filled with the studied mixture while the reference cell is filled with N_2. An experimental run is made of a 20 min isothermal step at 278.15 K followed by temperature scanning (0.5 K·min^{-1}) up to 333.15 K. Experiments were carried out at constant pressure (0.1 MPa) in both the sample and reference cells. The influence of the physical solvent on the specific heat capacities is shown in Figure X.7.

Figure X.7: Specific Heat Capacities as a function of temperature for the ternary systems {NMPD (w %) – TEG (w %) – H_2O (w %)}. $\bigcirc$, {NMPD (20) – TEG (0) – H_2O (80)}; ∇, {NMPD (20) – TEG (20) – H_2O (60)}; $\square$, {NMPD (20) – TEG (30) – H_2O (50)}; $\triangle$, {NMPD (20) – TEG (80) – H_2O (0)}. Numbers in brackets denote the weight percent of each mixture component. Dash lines are smooth fitting lines
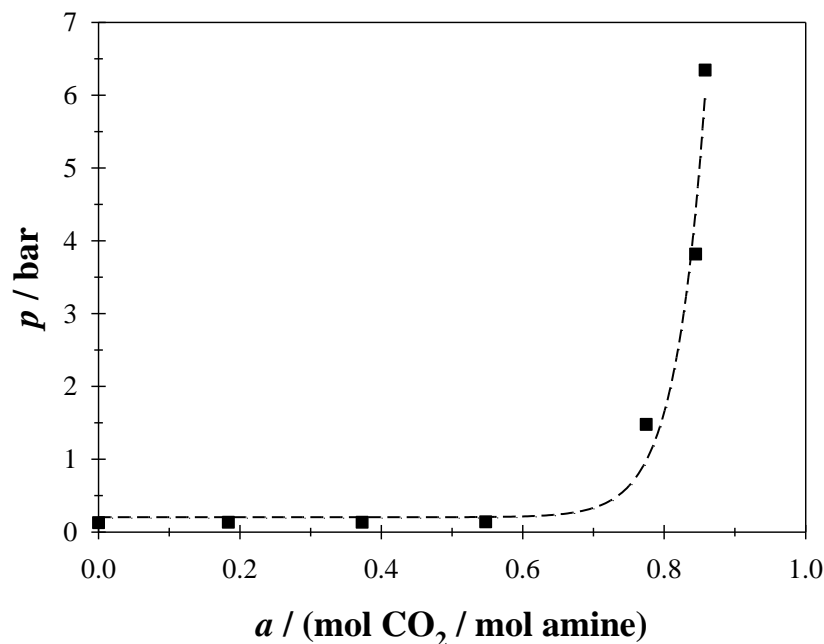
As expected, TEG reduces the heat capacities of the absorbent solution. The heat capacity is close to 2 $J.g^{-1}.K^{-1}$ when water is replaced by glycol as a solvent for the NMPD. This decrease is highly valuable for process design as the cost for heating the mixtures is drastically reduced with TEG.

X.5 Vapor-Liquid Equilibria of ternary systems {NMPD – TEG – H_2O – CO_2}

A specific description of the experimental device used in this work to measure VLE data has been reported by Zhang et al. [17]. Shortly, the technique of measurements is based on the "static-analytic" method described by Laugier and Richon [18] and experimental procedure is fully described in Coquelet and Richon [19]. With this apparatus both the liquid and vapor phases can be sampled under pressure using ROLSI™ capillary samplers [20, 21]. The equilibrium cell is immersed in a thermo-regulated liquid bath. In order to ensure accurate temperature measurements in the equilibrium cell and to check for thermal gradients, the temperature is measured at the top and bottom flanges through two 100 Ω platinum resistance thermometer probes. A variable-speed stirrer inside the cell accelerates the mass transfer

between phases and reduces the time needed to achieve equilibrium. Pressures are measured by three pressure transducers of which the maximum absolute pressures are 0.35 bar, 1 bar and 10 bar, respectively. Sample analysis is carried out by a gas chromatograph equipped with a thermal conductivity detector (TCD). After calibration the uncertainty on CO_2 composition in liquid phase is lower than 0.04.

Before measuring VLE, the equilibrium cell and its loading lines were first evacuated. About 30 mL of the mixture {NMPD (14) − TEG (17) − H_2O (69)} was introduced via a press at room temperature. The solution was then heated to 313 K. Meanwhile, an adequate stirring was maintained inside the cell. Phase equilibrium was assumed to be achieved while temperature and pressure readings stabilized for at least 30 min. The first pressure measurement gave the vapor pressure of the mixture investigated. Carbon dioxide was then loaded from a gas tank with controlled temperature and pressure. For each equilibrium condition, at least six samples of the liquid phase were withdrawn and analyzed to ensure composition repeatability within ±1%. CO_2 was then further introduced to measure the next equilibrium condition.
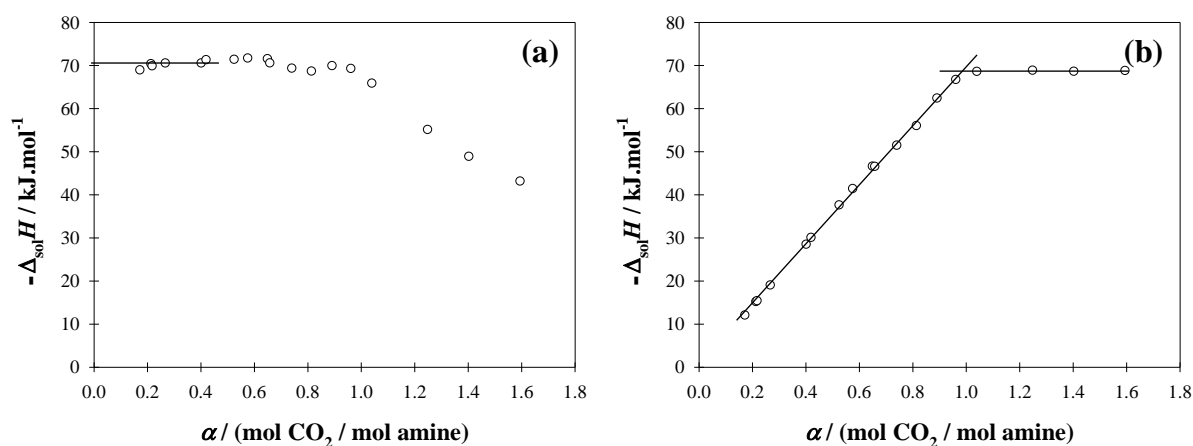

Figure X.8: Equilibrium pressure as a function of CO_2 loading charge for the system {NMPD (14) − TEG (17) − H_2O (69)} at 313 K. Numbers in brackets denote the weight percent of each mixture component.

The solubility of CO_2 in a solution of {NMPD (14) – TEG (17) – H_2O (69)} was determined at 313 K. Experiments were conducted for different CO_2 loading charges (α), up to the saturation of the absorbent solution and are illustrated in Figure X.8.

X.6 Enthalpies of Solution

The experimental setup used in this study has been carefully reported elsewhere [13]. Briefly, the enthalpy of solution of CO_2 in the ternary system {NMPD – H_2O – TEG} was measured by using a custom-made flow-mixing cell adapted to a Setaram BT2.15 heat conduction differential calorimeter. Experiments were carried out at constant temperature and pressure. The two fluids to be mixed (CO_2 and ternary solution) were injected into the flow lines by two high-pressure syringe pumps, thermo-regulated at near ambient temperature. Experiments were carried out at different loadings α (moles CO_2/mol amine). The gas loading charge is determined as described in the previous section.

Figure X.9: Enthalpy of solution ($-\Delta_{sol}H$) versus CO_2 loading charge for an aqueous solution {NMPD (20) – TEG (20) – H_2O (60)}at T = 313 K and p= 1.0 MPa. (a) $\Delta_{sol}H/$(kJ mol^{-1} of CO_2), straight lines show the average values for the enthalpies of solution at low loadings ($\alpha < 0.5$); (b) $\Delta_{soln}H/$(kJ mol^{-1} of NMPD).

Enthalpies of solution of CO_2 in solutions of {NMPD – H_2O – TEG} were measured at 313 K at pressure of 1 MPa, for two absorbent mixtures (w_{NMPD} = 0.20, w_{TEG} = 0.20). Experiments were conducted for different loading charges (α), up to the saturation of the absorbent solution. As an example, experimental enthalpies measured for {NMPD – H_2O – TEG} and expressed in kJ.mol^{-1} of CO_2 (Fig. X.9.a) and of NMPD (Fig. X.9.b) have been plotted versus

loading charge α (mol of CO_2/mol of amine). . In Fig. X.9.a, the enthalpies of solution for CO_2 are exothermic and equivalent, up to a loading charge of 0.5.The average enthalpy values $\Delta_{sol}H^{av}$, for $\alpha < 0.5$ is found to be -71.5 kJ.mol^{-1}. These values were not determined for the binary system {NMPD – H_2O} with $w_a = 0.2$ because phase separations would occur while adding CO_2 in this experimental condition of temperature (Figure X.5). In Fig. X.9.b, experimental enthalpies of solution expressed in kJ.mol^{-1} of NMPD show two different domains. In the first domain ($0 < \alpha < 1$), $\Delta_{sol}H$ increases linearly with the loading charge. The value of the slope in this domain is equal to $\Delta_{sol}H^{av}$ obtained previously (Fig. X.9.a). The second domain where the enthalpy of solution stays constant is characteristic of a saturated solution. The intersection between unsaturated (enthalpy increase) and saturated (plateau) domains yields the solubility limit (s). The experimental solubility limit of CO_2 in the ternary system {NMPD – H_2O – TEG} was graphically determined at 313 K and 1.0 MPa

X.7 Discussion and Conclusion

A part of the thermodynamic properties required (phase diagram, heat capacity, heat of absorption, density) for the design of the new operation units for CO_2 removal have been determined in this study. These preliminary results show the substantial benefits of the addition of a physical solvent to an aqueous solution of amine. Among these advantages, the specific heat capacities of liquid phases can be lowered allowing energy savings, and the temperatures of the phase separation in the presence of CO_2 can be controlled. Nevertheless, additional thermodynamic data (such as Henry constant) are needed to complete this study, in order to develop a reliable thermodynamic model that takes into account the mechanism of reaction of CO_2 with the amine and the formation of electrolytes species. For that purpose an original device developed by Provost *et al.* [22] allowing the simultaneous measurements of the pressure and liquid phase composition, as a function of time will be used. The liquid phase composition is evaluated through the analysis FT-IR spectrum, recorded in situ with an ATR accessory.

In addition to this, thermodynamics models developed by Paricaud *et al.* [23] will be applied to these systems and could run within process simulation software. The first step will be the development of a thermodynamic model for electrolyte solutions, which considers the most important chemical species in the aqueous and amine solutions, and is able to predict the liquid-liquid immiscibility as well as the chemical and phase equilibria. This model will be

used to describe both the phase equilibria and energetic properties such as heat capacities. I will be implemented into a code that is compatible with the CAPE-OPEN interface of Simulis Thermodynamics® and prosim plus® software developed by the Prosim company. Through this interface, we will be able to simulate the main three elements of the separation process (decanter and absorption and desorption columns) in either the Prosim plus® or Aspen one® environment, and estimate the cost and energy requirement for the CO_2 capture.

X.8 Acknowledgment

REFERENCEs

1. Zhao, Q., Leonhardt, E., MacConnell, C., Frear, C., and Chen, S., *Purification technologies for biogas generated by anaerobic digestion.* 2010. p. 1-24.
2. Rochelle, G.T., *Amine Scrubbing for CO2 Capture.* Science, 2009. 325(5948): p. 1652-1654.
3. Raynal, L., Bouillon, P.-A., Gomez, A., and Broutin, P., *From MEA to demixing solvents and future steps, a roadmap for lowering the cost of post-combustion carbon capture.* Chemical Engineering Journal, 2011. 171(3): p. 742-752.
4. Raynal, L., Briot, P., Dreillard, M., Broutin, P., Mangiaracina, A., Drioli, B.S., Politi, M., La Marca, C., Mertens, J., Thielens, M.-L., Laborie, G., and Normand, L., *Evaluation of the DMX Process for Industrial Pilot Demonstration – Methodology and Results.* Energy Procedia, 2014. 63: p. 6298-6309.
5. Raynal, L., Alix, P., Bouillon, P.-A., Gomez, A., le Febvre de Nailly, M., Jacquin, M., Kittel, J., di Lella, A., Mougin, P., and Trapy, J., *The DMX™ process: An original solution for lowering the cost of post-combustion carbon capture.* Energy Procedia, 2011. 4(0): p. 779-786.
6. Ballerat-Busserolles, K., Lowe, A.R., Coulier, Y., and Coxam, J.Y., *Calorimetry in Aqueous Solutions of Demixing Amines for Processes in CO2 Capture*, in *Acid Gas Extraction for Disposal and Related Topics.* 2016, John Wiley & Sons, Inc. p. 69-80.
7. Fandiño, O., Yacyshyn, M., Cox, J.S., and Tremaine, P.R., *Speciation in Liquid-Liquid Phase-Separating Solutions of Aqueous Amines for Carbon Capture Applications by Raman Spectroscopy*, in *Acid Gas Extraction for Disposal and Related Topics.* 2016, John Wiley & Sons, Inc. p. 81-94.
8. Dash, S.K. and Bandyopadhyay, S.S., *Studies on the effect of addition of piperazine and sulfolane into aqueous solution of N-methyldiethanolamine for CO2 capture and VLE modelling using eNRTL equation.* International Journal of Greenhouse Gas Control, 2016. 44: p. 227-237.
9. Zheng, C., Tan, J., Wang, Y.J., and Luo, G.S., *CO2 Solubility in a Mixture Absorption System of 2-Amino-2-methyl-1-propanol with Ethylene Glycol.* Industrial & Engineering Chemistry Research, 2013. 52(34): p. 12247-12252.
10. Coulier, Y., Ballerat-Busserolles, K., Rodier, L., and Coxam, J.Y., *Temperatures of liquid–liquid separation and excess molar volumes of {N-methylpiperidine–water} and {2-methylpiperidine–water} systems.* Fluid Phase Equilibria, 2010. 296(2): p. 206-212.
11. Stephenson, R.M., *Mutual solubility of water and pyridine derivatives.* Journal of Chemical & Engineering Data, 1993. 38(3): p. 428-431.
12. Coulier, Y., Lowe, A.R., Moreau, A., Ballerat-Busserolles, K., and Coxam, J.-Y., *Liquid-Liquid Equilibria in {Amine - H_2O - CO_2} Mixtures: New Methods for Key Data.* Fluid Phase Equilibria, 2016. accepted.
13. Arcis, H., Ballerat-Busserolles, K., Rodier, L., and Coxam, J.-Y., *Enthalpy of Solution of Carbon Dioxide in Aqueous Solutions of Monoethanolamine at Temperatures of 322.5 K and 372.9 K and Pressures up to 5 MPa.* Journal of Chemical & Engineering Data, 2011. 56(8): p. 3351-3362.
14. Span, R. and Wagner, W., *A New Equation of State for Carbon Dioxide Covering the Fluid Region from the Triple-Point Temperature to 1100 K at Pressures up to 800 MPa.* Journal of Physical and Chemical Reference Data, 1996. 25(6): p. 1509-1596.
15. Coquelet, C., Valtz, A., Courtial, X., and Richon, D., *Volumetric properties of the water + 3-(dimethylamino) propylamine (DMAPA) mixture at atmospheric pressure from 283.15 to 353.15 K.* Thermochimica Acta, 2006. 448(1): p. 47-51.

16.   Coulier, Y., Ballerat-Busserolles, K., Mesones, J., Lowe, A., and Coxam, J.-Y., *Excess Molar Enthalpies and Heat Capacities of {2-Methylpiperidine–Water} and {N-Methylpiperidine–Water} Systems of Low to Moderate Amine Compositions.* Journal of Chemical & Engineering Data, 2015. 60(6): p. 1563-1571.

17.   Zhang, F., Théveneau, P., El Ahmar, E., Canet, X., Soo, C.-B., and Coquelet, C., *An improved static–analytic apparatus for vapor–liquid equilibrium (PTxy) measurement using modified in-situ samplers.* Fluid Phase Equilibria, 2016. 409: p. 425-433.

18.   Laugier, S. and Richon, D., *New apparatus to perform fast determinations of mixture vapor–liquid equilibria up to 10 MPa and 423 K.* Review of Scientific Instruments, 1986. 57(3): p. 469-472.

19.   Coquelet, C. and Richon, D., *Chapter 14 Solubility of BTEX and Acid Gases in Alkanolamine Solutions in Relation to the Environment*, in *Developments and Applications in Solubility*. 2007, The Royal Society of Chemistry. p. 219-235.

20.   Guilbot, P., Valtz, A., Legendre, H., and Richon, D., *Rapid on-line sampler-injector: a reliable tool for HT-HP sampling and on-line GC analysis.* Analusis, 2000. 28(5): p. 426-431.

21.   Théveneau, P. and Legendre, H., *Dispositif pour prélever des micro-échantillons d'un fluide à l'état liquide contenu dans un containeur*. 2014, French Patent Application No. 1460309.

22.   Diab, F., Provost, E., Laloué, N., Alix, P., Souchon, V., Delpoux, O., and Fürst, W., *Quantitative analysis of the liquid phase by FT-IR spectroscopy in the system CO2/diethanolamine (DEA)/H2O.* Fluid Phase Equilibria, 2012. 325: p. 90-99.

23.   Fukumoto, A., Sales Silva, L.P., Paricaud, P., Dalmazzone, D., and Fürst, W., *Modeling of the dissociation conditions of H2 + CO2 semiclathrate hydrate formed with TBAB, TBAC, TBAF, TBPB, and TBNO3 salts. Application to CO2 capture from syngas.* International Journal of Hydrogen Energy, 2015. 40(30): p. 9254-9266.